geologicaacta

Citation: Canales-García, I., Pérez-Cruz, G., Orozco-Almazán, L., Urrutia-Fucugauchi, J., 2025. Basement Structural Controls on the Jurassic Sedimentary Sequences in the Tampico-Misantla Basin, Northeastern Mexico from a 3-D Seismic Reflection Study. Geologica Acta, 20.21, 1-pgs. DOI: 10.1344/2025.23.21

Online ISSN: 1696-5728

Basement Structural Controls on the Jurassic Sedimentary Sequences in the Tampico-Misantla Basin, Northeastern Mexico from a 3-D Seismic Reflection Study

Iza Canales-García[1] Guillermo Pérez-Cruz[1] Liz Orozco-Almazán[1,2] Jaime Urrutia-Fucugauchi[3, 4*]

[1]División de Ingeniería en Ciencias de la Tierra, Facultad de Ingeniería, Universidad Nacional Autónoma de México
Coyoacán 04510, México, México

[2]Programa de Posgrado Ciencias del Mar y Limnología, Universidad Nacional Autónoma de México
Coyoacán 04510, México, México

[3]Programa Universitario de Perforaciones en Océanos y Continentes, Instituto de Geofísica, Universidad Nacional Autónoma de México
Coyoacán 04510, México, México

[4]Instituto de Investigación Científica y Estudios Avanzados Chicxulub, Parque Científico Tecnológico de Yucatán, Sierra Papacal
Mérida 97302, Yucatán, México

*Corresponding author; E-mail juf@igeofisica.unam.mx

ABSTRACT

The Tampico-Misantla basin is a mature oil rich province in northeastern Mexico with large unconventional oil plays currently being explored. Results of a 3-D seismic reflection study of the basement and Jurassic sequences are used to analyze the basement influence on the sedimentary sequence and basin structure, by mapping the seismo-stratigraphic horizons for the (Tithonian) Pimienta, (Kimmeridigian) Taman/San Andrés, (Oxfordian) Santiago, (Callovian) Tepexic/Huehuetepec and (Bathonian) Cahuasas formations. The basement is characterized by stepped NW-SE tilted blocks of horst and grabens. The horst sections to the northeast are found at depths of 3200 m and get deeper up to 6500 m to the southwest. Blocks bounded by planar curved high angle normal faults with NW-SE and NE-SW orientation form a Triassic-Jurassic system, with two major pulses during the Bajocian and Oxfordian. Vertical slips of main faults are variable and may reach 2000 m. Basement blocks play major roles in defining the depositional processes, with thickness and distribution of overlying sedimentary units. Based on our analysis the Middle Jurassic Cahuasas Formation units were deposited predominantly in continental environments and exhibit large thickness variations. The Callovian Tepexic and Huehuetepec Formations were deposited in transitional and shallow marine environments, with relatively uniform thickness and distribution. The Oxfordian to Tithonian Santiago, Taman/San Andres and Pimienta Formations were deposited in marine environments, showing multiple fault deformation with tendency of progressively pinching out against the topographic highs. The thickness variation in the Santiago Formation suggests episodes of increasing subsidence and fault reactivation. The seismic volume models constraint the basement structures and Jurassic sequence stratigraphy in the Tampico-Misantla basin.

KEYWORDS | **Seismic modeling, Basement, Tectono-stratigraphic evolution, Tampico-Misantla basin, Jurassic, Northeastern Mexico**

INTRODUCTION

The Tampico-Misantla basin forms part of the northeast and eastern central Mexico oil and gas provinces (Fig. 1). The northeast oil provinces have been long studied, including the discoveries in the early 1900's and the oil producing fields. The basin has had an important production of the order of 6.2 billion Barrels of Oil Equivalent (BOE), with major reserves from different hydrocarbon systems (Guzman, 2022; Guzman-Vega *et al.*, 2001; Magoon *et al.*, 2001). The unconventional plays have potential reserves of more than 100 billion BOE that have not been developed (Guzman, 2022).

Hydrocarbon source systems include the Tithonian Pimienta Formation that presents a high oil and wet gas potential (Guzman-Vega *et al.*, 2001; Jarvi and Maende, 2016) Interest has increased in recent years with the exploration of unconventional resources of shale oil and gas and coal-bed gas (Guzman, 2022; Vega-Ortiz *et al.*, 2020). Studies so far have focused on the geological characterization of the sedimentary sequences, reservoirs, seals, oil traps, migration and the petroleum systems (Abascal-Hernandez *et al.*, 2018; Busch and Govela, 1978; Jarvie, 2012; Guzman, 2022; Maende, 2016; Morelos-Garcia, 1996). Detailed geophysical studies are needed for the exploration programs.

The area of northeastern Mexico has a complex geological evolution, associated to the opening of the Gulf of Mexico. It experienced a major compressive deformation during the Late Cretaceous-middle Eocene, with the development of the Sierra Madre Oriental fold and thrust belt (Fitz-Diaz *et al.*, 2018; Gray *et al.*, 2001; Van Avendock *et al.*, 2015). In the basin, four tectonic stages have been recognized, 1) a rifting stage during which Triassic to middle Jurassic continental sedimentary sequences were deposited, 2) a passive margin stage when deposition of upper Jurassic to upper Cretaceous marine sequences occurred, 3) an upper Cretaceous to early Eocene stage of foreland basin during which mainly marine clastic sequences were deposited and 4) a passive margin when late Eocene to Recent clastic sequences deposited.

The study aims to investigate the structure and stratigraphy on a Tampico-Misantla basin sector, with emphasis on the basement and Jurassic sedimentary sequences. We analyze a 3-D seismic reflection volume to characterize the systems of horsts and grabens developed during the late Triassic-middle Jurassic rifting and the stratigraphic sequences.

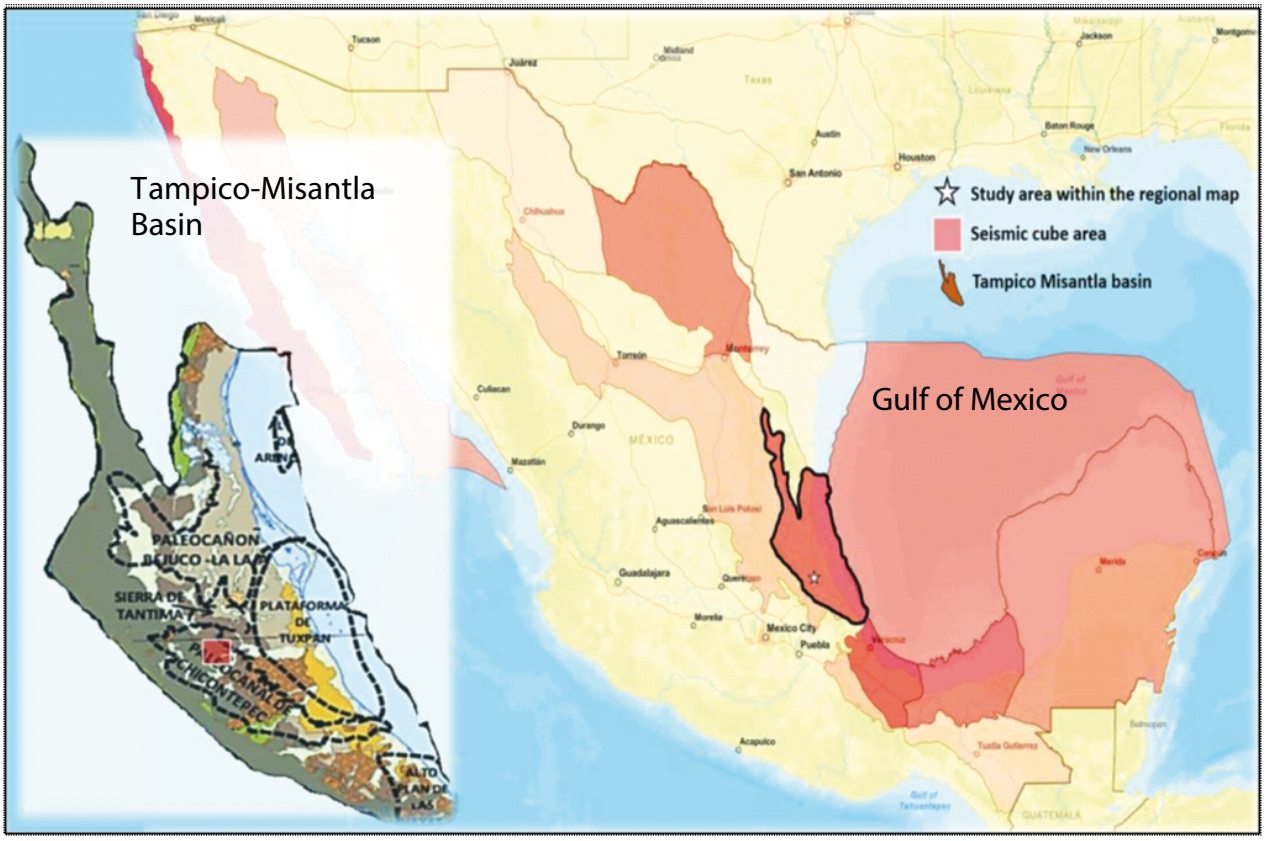

FIGURE 1. Location of the Tampico-Misantla basin. It shows the approximate location of the seismic cube in a red box.

BASEMENT AND STRATIGRAPHY

Basement

The geology of the Tampico-Misantla basin has been long investigated, mainly as part of the exploration programs and hydrocarbon potential (*e.g.* Bonet, 1956; Busch and Govela, 1978; Goldhammer, 1999; Guzman, 2022; Heim, 1926, 1940; Hermoso de la Torre and Martinez-Perez, 1972; Muir, 1936; Lopez Ramos, 1979). The Triassic to recent stratigraphic sequences, up to 6500m depths, overlie a Permo-Triassic basement (Fig. 2). Basement consists of an igneous metamorphic complex composed of schists and granodiorites (López Infanzón, 1986; Ranson *et al.*, 1982; Wilson, 1986). North and west of the study area several wells cut metamorphosed arkose of undefined age at depths of about 2500m, underlying upper and middle Jurassic sedimentary rocks (Petroleos Mexicanos, 1988).

Depths of the basement based on gravity and magnetic data (Comision Nacional de Hidrocarburos, 2018) recognize a regional trend of highs (altos) and lows (fosas) running parallel to the Sierra Madre Oriental (SMO) tectonic front. This trend extends from the Sierra de Tamaulipas in the north to Tezuitlan, Puebla in the south. Highs and lows can be interpreted as horst and grabens, which conform a late Triassic~mid Jurassic continental rift system (Comision Nacional de Hidrocarburos, 2018; Goldhammer and Johnson, 2001; Magoon *et al.* 2001; Salvador, 1987, 1991).

In map view, individual blocks are distributed mainly normal to the axial regional structure. Depths to basement in some grabens, *i.e.* fosa de Planos, reach 7200m below the surface. The study area lies in the northern sector of the fosa de Planos between the Alto de Tuxpan and the SMO tectonic front. The conceptual Jurassic geologic model, with the sedimentary sequences deposited on the regional system of basement horst and grabens is shown in Figure 3.

Stratigraphy

The basin stratigraphy has long been investigated as part of geological/geophysical surveys and oil exploration projects (Fig. 2; Aguilera, 1972; Goldhammer and Johnson, 2001; Medina, 2023; Petroleos Mexicanos, 1988). At the end of the Triassic and into the early Jurassic, continental clastic sediments of alluvial and fluvial environments were deposited with lava flows. The Huayacocotla Formation of lower Jurassic Toarcian Hettangian-Pliensbachian age was formed by a sequence of marine, transgressive sandstones and shales. During the middle Jurassic, continental conditions were reestablished with deposition of Cahuasas Formation. At the end of this period, a marine transgression initiated, favoring the deposition of evaporitic sediments and oolitic limestones of the Huehuetepec Formation (Callovian), and

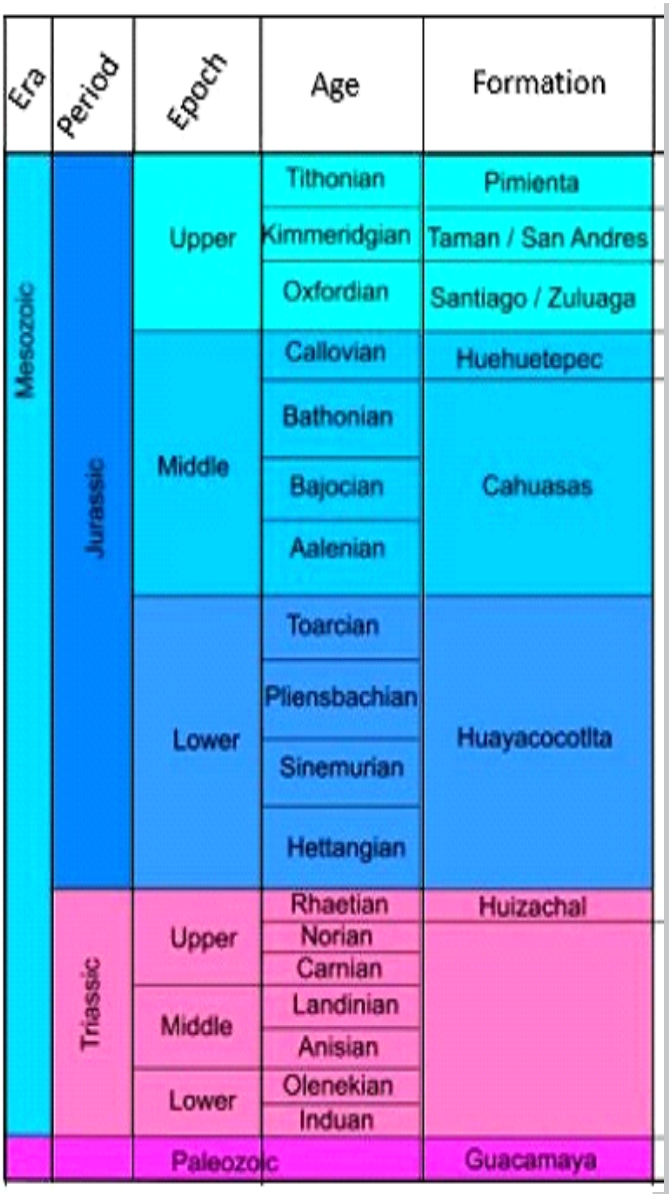

FIGURE 2. Generalized stratigraphic column (modified from Medina, 2023; Comision Nacional de Hidrocarburos, 2018).

sandy limestones with bioclasts and oolites of the Tepexic Formation (Callovian) which overlaid calcareous and carbonaceous shales with abundant organic matter of the Santiago Formation (Oxfordian). Deposits are in low energy environments as the marine transgression progressed, over paleogeographic highs, with carbonate ramps developed on which shaly limestones and oolitic limestones of the San Pedro and San Andrés Formations (Kimmeridgian). Their lateral equivalents consist in shaly limestones with few bioclasts and oolites of Chipoco Formation and black shales and limestones of Tamán Formation. The conditions of transgressive seas continued, and during the Tithonian, a transgression occurred covering basement inherited paleogeographic highs. During this time, shaly, organic rich

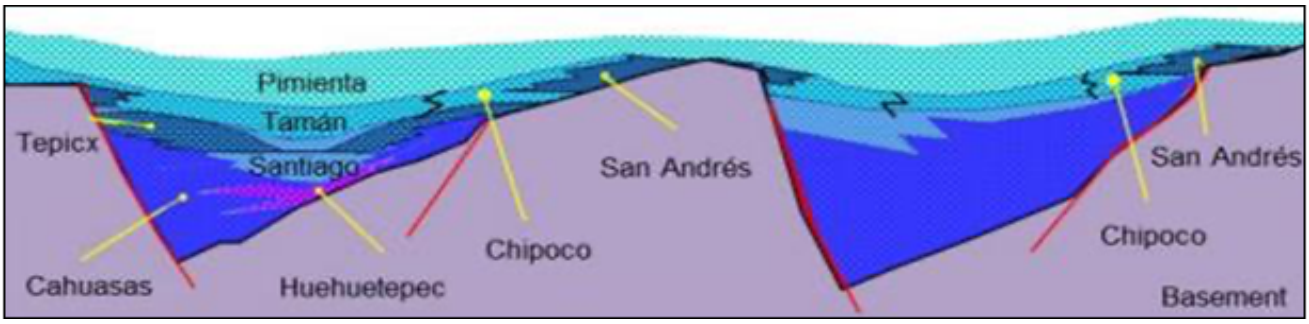

FIGURE 3. Schematic cross-section of basement and Jurassic sequences in the Tampico-Misantla basin. The structure is characterized by grabens and horsts (taken from the Geological Atlas of the Tampico-Misantla basin; Comision Nacional de Hidrocarburos, 2018).

limestones of the Pimienta Formation were deposited in a relatively open marine environment (Abascal-Hernandez *et al.*, 2018; Aguilera, 1972).

DATA AND METHODS

We used a depth-migrated seismic volume to extract a Relative Acoustic Impedance volume and used both for the interpretation (Assis *et al.*, 2019; Gray *et al.*, 2001; Karimi, 2015). The top of the basement plus five key stratigraphic seismic horizons are mapped. The horizons correspond to the tops of the widespread Jurassic stratigraphic units: Pimienta (Tithonian), Taman (Kimmeridgian), Santiago (Oxfordian), Tepexic (Callovian), and Cahuasas (Aalenian to Bathonian) Formations. Normal faults identified are correlated along the volume. The stratigraphic information derived from three wells that penetrated the Jurassic column provide constraints on the top of the stratigraphic units (Fig. 4).

For further characterization and analysis of the seismic volume, seismic attributes are used. Seismic attributes provide useful constraints on the reflector packages and physical property contrasts (Chopra and Marfurt, 2005, 2018; Marfurt, 2007; Salguero-Hernandez *et al.*, 2020). Root Mean Square (RMS) amplitude and variance attributes calculated from the 3-D seismic grid at different depth horizons are used to constrain the structure and stratigraphy of the seismic volume. Changes in signal-noise ratio determined from RMS attribute allow investigating noise, structural and stratigraphic zoning (Marfurt, 2007). The variance attributes measure how similar given waveforms are, constraining the vertical and lateral reflector coherency for seismic volumes. Variance attributes permit enhancing structural and stratigraphic discontinuities (Chopra and Marfurt, 2018).

The RMS and variance attributes are calculated in the seismic cubes at 6, 5.2, 3.7, 3.5 and 3km cut-off depths. For structural analysis, the volume attributes are then correlated with the seismic horizons for the basement and the top of the Oxfordian, Kimmeridgian and Tithonian formations (Orozco Almazan, 2021).

From the interpreted horizons and faults, the structural maps and models were used to infer distribution, thickness and environments of mapped units. Inferences about paleogeography and timing of structural deformation are proposed, with the implications of seismic stratigraphy for the regional tectono-stratigraphic evolution (Goldhammer *et al.*, 1991).

Zones of tilted blocks, faults and folds show high complexity, with structures formed during early tectonic events and then modified by a later one. The structural interpretation of the basement top is made marking the deepest seismic events below which, seismic information degrades drastically (acoustic basement). The structures corresponding to the late Cretaceous folding and thrusting are interpreted from the seismic images, with the integrated stratigraphic and structural data constraining the geometry

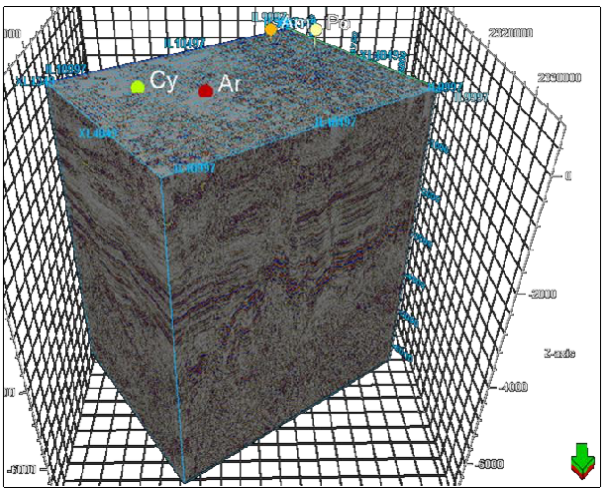

FIGURE 4. The seismic cube analyzed, with the location of the wells used for stratigraphic correlation.

and extension of sedimentary units (Aguilera, 1972; Goldhammer *et al.*, 1991).

RESULTS

Seismic Interpretation

The seismic profiles across the volume are used to interpret the horizons and faults and construct structural maps. The sequence is formed by upper and lower reflective units and an intermediate transparent unit. The horizons associated with upper Jurassic markers Tithonian, Kimmeridgian and Oxfordian are related to continuous, undulating reflections of low amplitude. Faults limit horst and grabens, like the Camaitlán-Tlacolula horst and the Ayacaxtla graben (Figs. 5; 6). Offsets of faults are variable and may reach up to 2000m. Faults extend upward and cut upper Jurassic and Cretaceous units. Some faults were reactivated during the Laramide orogeny (Fitz-Diaz *et al.*, 2018).

Profile I in a SW-NE direction is perpendicular to the SMO regional front (Fig. 5). For the basement two cases are analyzed: case 1 considers a shallow basement immediately underneath the Bajocian Cahuasas horizon, whereas case 2 considers a deep basement averaging 2000m below the Bajocian horizon (less in rift shoulders). The basement horizon at the base of the sedimentary sequence and top of the igneous metamorphic complex is marked by variable amplitude and discontinuous seismic events that in some zones tend to be parallel to the Callovian Tepexic and Bajocian Cahuasas horizons. This horizon is accompanied by a couple of strong amplitude reflections. Locally, the characteristic seismic event is immersed in high frequency noise or is absent, making interpretation speculative. The stratigraphic column between the Cahuasas and basement seismic horizons includes Bajocian to late Triassic rocks of continental origin and shallow marine lower Jurassic rocks of the Huayacocotla Formation. Seismic facies between the two horizons tend to be chaotic and a rather transparent package, although in some regions, facies of high amplitude and coherent parallel reflections can be observed. For the analysis the deep basement case is adopted.

Considering the distribution and lateral thickness variations of the stratigraphic units constrained by the interpreted horizon, we acknowledge that deposition of lower and early middle Jurassic units took place during an active process of rifting, whereas those of the upper Jurassic were deposited under conditions of reduced tectonic activity dominated by thermal subsidence (Van Avendock *et al.*, 2015). The structures of Jurassic horizons are influenced by the basement geometry.

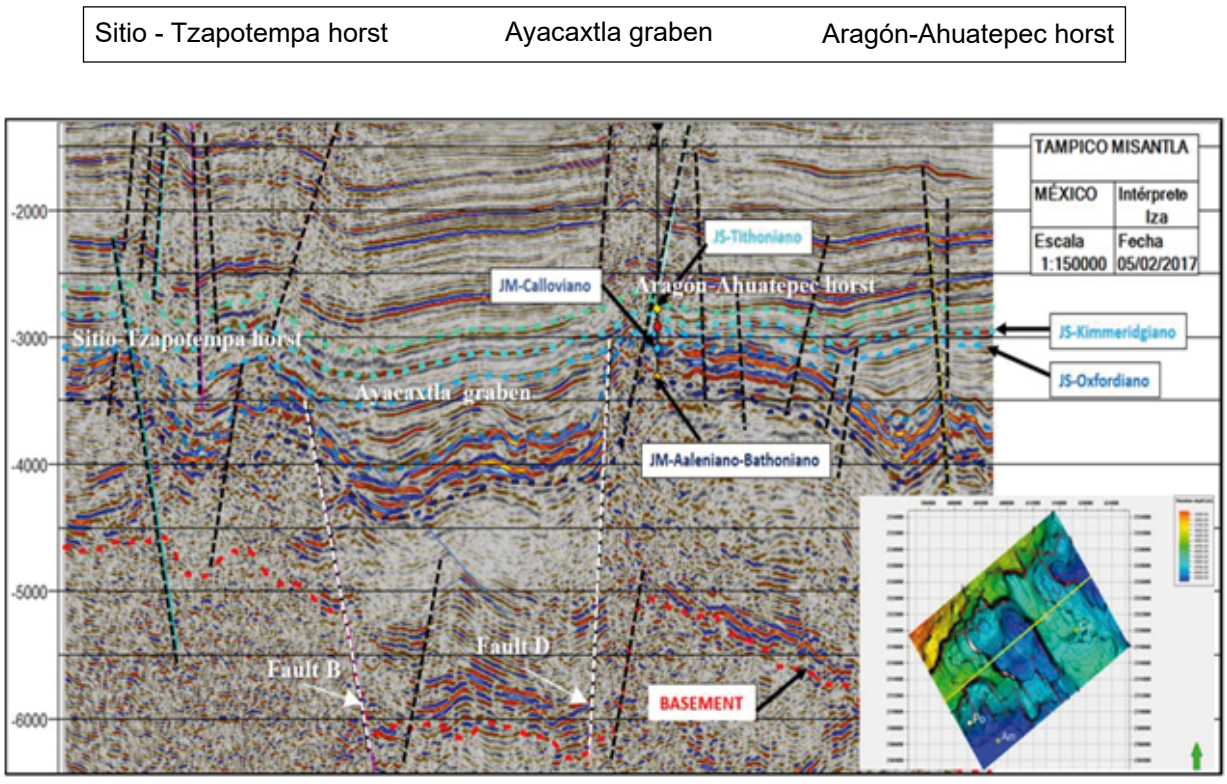

FIGURE 5. SW-NE seismic section. The interpretation of six seismic horizons and the fault systems thllow line.

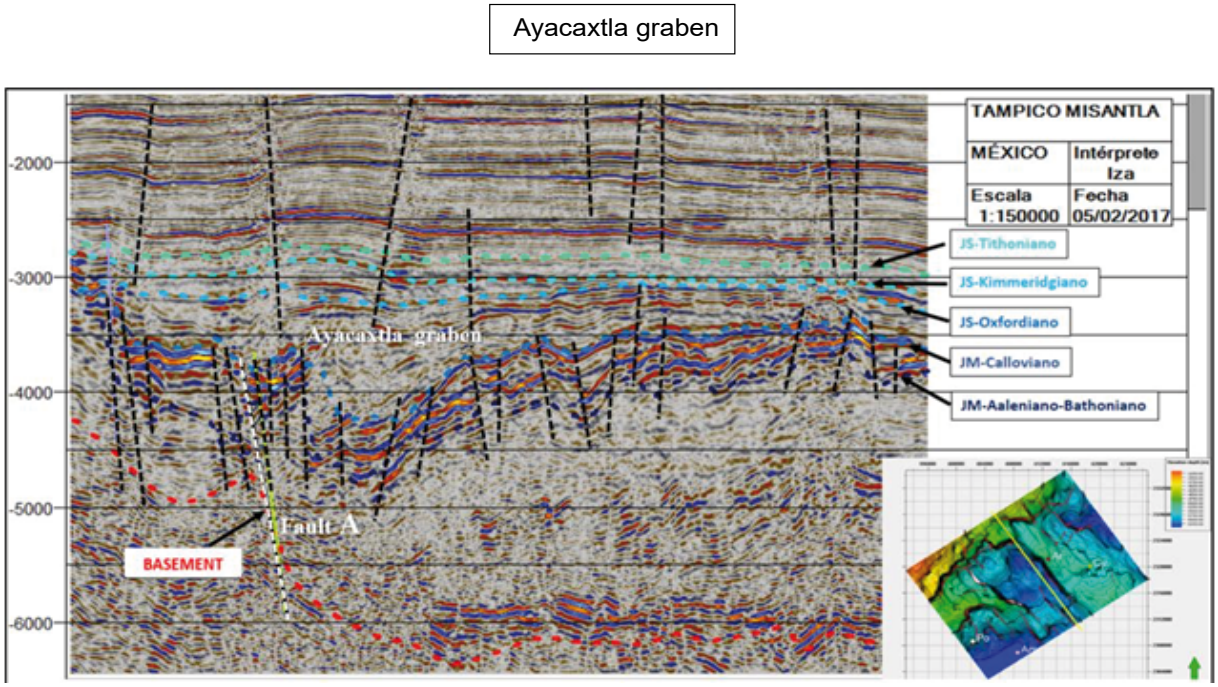

FIGURE 6. SNW-SE seismic section. The interpretation of six seismic horizons and the fault systems that affect them are observed. The structural map shows the location of Profile II with a yellow line.

Profile II in the NW-SE direction is parallel to the Sierra Madre Oriental front (Fig. 6). Structures in this profile include the Ayacaxtla graben, Camaitlán-Tlacolula horst and domino-like system of normal faults affecting Callovian and Bajocian horizons with hanging blocks to the NE. Following, map view descriptions of structures are associated with interpreted horizons, combined with the depositional patterns of units in between.

Basement

The regional structure is formed by a system of horst and grabens, which controls the carbonate sedimentation (Wilson, 1986). Horsts include the SW-NE Camaitlán-Tlacolula horst in the north, the WNW-ESE Sitio-Tzapotempa horst in the west and NW-SE Aragón-Ahuatepec horst in the east (Fig. 7). The horsts are separated by three grabens, from west to east, Amatitlán (deepest), Ayacaxtla and Coyotes. The basement horizon exhibits irregular relief, with elevated zones up to 3,300m deep in the horsts and up to 6,500m or more in the grabens. The faults that limit horst from grabens are high angle, planar with vertical slips that may reach up 2000m. Although there are numerous faults that cut the basement, for the present analysis some were chosen, identified as A, B, C and D. Fault A formed by various segments of gentle curvature put in contact the Camaitlán-Tlacolula horst with the other horst and grabens. Fault B with strong curvature forms the southern limit of the Sitio-Tzapotempa horst, whereas fault C forms its eastern limit. Fault D in the western limit of the Aragon-Ahuatepec horst is planar and steep. Faults were active since the Triassic to upper Jurassic, with two major pulses, one during lower and middle Jurassic and another during Oxfordian This set of structural elements resulted in a complex mosaic of NW-SE and SW-NE tilted blocks.

Cahuasas (Bajocian)

In the structural map of the Bajocian Cahuasas horizon, structures follow the basement (Fig. 8); with departures like the Aragón-Ahuatepec horst that gets wider to the south

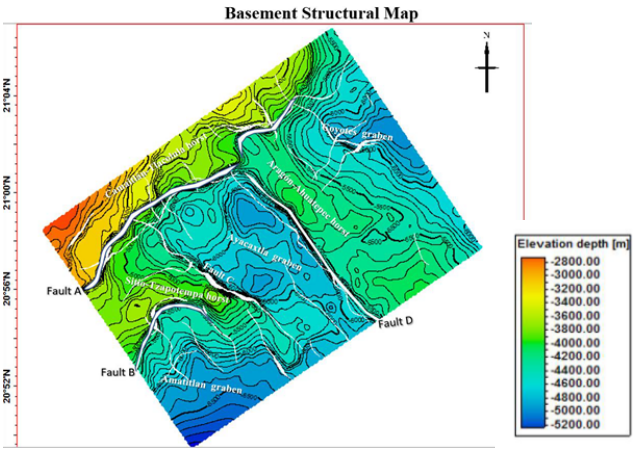

FIGURE 7. Structural map of the basement. Fault polygons are shown in white. Scale 1–1400000, contour increments 100.

and separation in two blocks in the Camaitlán-Tlacolula horst. The depths vary from 2,800m to 5,200m.

Sedimentation in grabens is mostly derived from erosion of elevated topographic highs, with siltstones, sandstones, and conglomerates in alluvial fans, fluvial and lacustrine environments. Deposition continued as long as the rift remained active. Large thickness variations are observed from block to block. The sequence between the basement and the Cahuasas horizons is approximately 500m thick in the NW and over 2500m in the SE.

Tepexic (Callovian)

Structural features of the Tepexic horizon are similar to those observed in the basement and Cahuasas horizons, with reduced relief which varies from 2,600 to 4,600m (Fig. 9). It is important to acknowledge that there are two stratigraphic units within the Cahuasas and the Tepexic horizons: the Huehuetepec Formation at the base, and the Tepexic formations at the top. The Huehuetepec Formation in outcrops south of the study area, contains layers of salt, anhydrites and red siltstones interdigitated with layers of limestones and calcarenites deposited in sabkha and ramp settings, with total thickness of 150m (González-García, 1970).

The Tepexic Formation consists of intercalated layers of dark shales, shaly limestones and calcarenites, oolites and bioclasts with total average thickness of 20m. In the study area, based on our seismic analysis and well control, the total thickness of both formations varies from 200 to 800m. These type of deposits records first pulses of marine invasion into the basin. The seismic character of the interval consists of high amplitude, partially undulated,

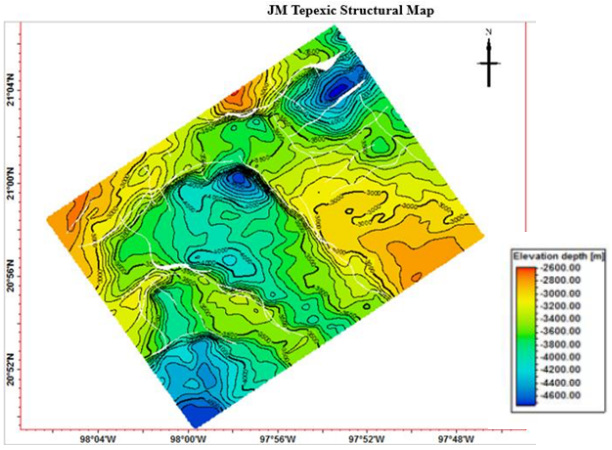

FIGURE 9. Structural map of the top of the Tepexic Formation. Scale 1–1400000, contour increments 100.

discontinuous events that extend along the study area. The undulated nature in the southwest is associated in part with Laramide folding. Based on the distribution, lateral thickness and proposed depositional environments of these stratigraphic units, they were deposited once the rifting episode had ceased.

Santiago (Oxfordian)

The map of the Santiago horizon retains some of the structural features and tendencies observed on previous maps but more attenuated (Fig. 10). The relief along the study area varies from 2,600 to 3,600m. The interval between the Callovian and Santiago horizons contains the Santiago Formation that includes a sequence of black calcareous shales intercalated with gray shaly limestones deposited in an open marine environment (Cantú-Chapa,

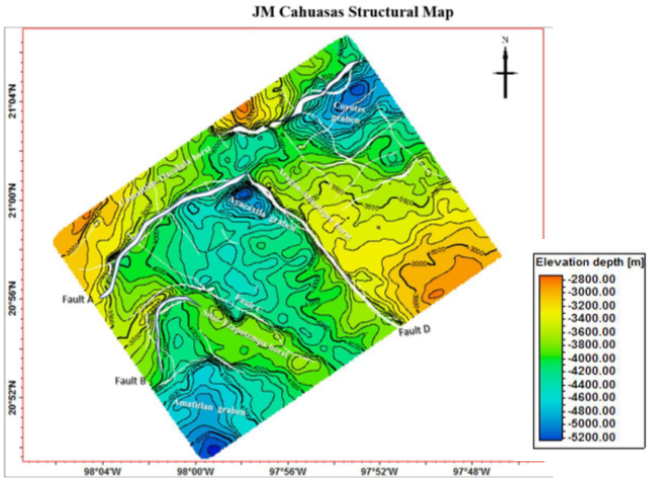

FIGURE 8. Structural map of the top of the Cahuasas Formation. Scale 1–1400000, contour increments 100.

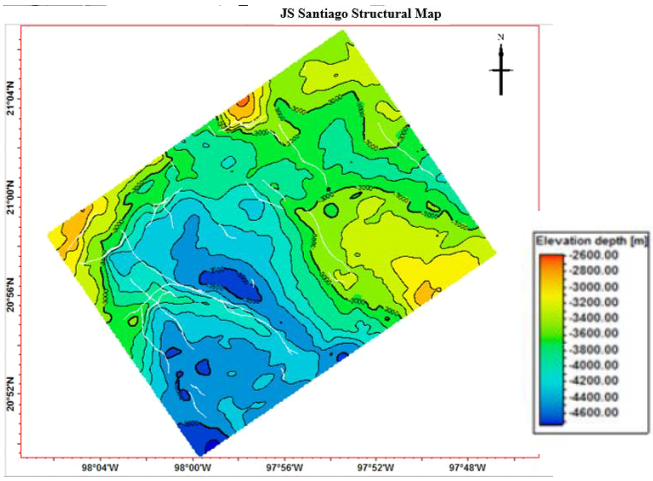

FIGURE 10. Structural map of the top of the Santiago Formation. Scale 1–1400000, contour increments 100.

1969, 1984). In the study area its thickness varies from 0 to 700m, thicker deposits are present in zones of low relief like the Ayacaxtla and Coyotes depressions. This sedimentary sequence pinches out on Sitio-Tzapotempa and Aragón-Ahuatepec highs with gentle folding in the southwestern sector. Faults of the rift system reactivated, extending upward. Thickness variations of the Santiago Formation suggest an episode of fault reactivation and subsidence in a passive margin regime.

Taman and Pimienta (Kimmeridgian and Tithonian)

Kimmeridgian and Tithonian horizons appear similar and maintain some of the structural features and tendencies observed previously but attenuated (Figs. 11; 12). Depths to the Taman horizon vary from 2,600 to 3,400m, whereas those of the Tithonian, from 2,500 to 3,200m (Fig. 11). The interval between Santiago and Pimienta horizons spans the Taman and Pimienta Formations. These two horizons are almost parallel to each other. Thickness of Taman Formation varies from 0 to 350m (Fig. 11). Thickness of the Pimienta from 0 to 300m (Fig. 12). Both formations tend to pinch out against the flanks of remanent highs, as the Aragón-Ahuatepec and Camaitlán-Tlacolula. Gentle folds with axis parallel to the SMO tectonic front are present in the southwestern area, with some cut at their flanks by reverse faulting of small displacement extending upwards into the Cretaceous units.

The Taman Formation is correlative in age to San Andres and Chipoco Formations, which developed in open marine basin, ramps, and shallow platforms, respectively. The San Andres Formation contains layers of oolitic limestones and calcarenites, whereas the Chipoco Formation contains intercalations of crystalline

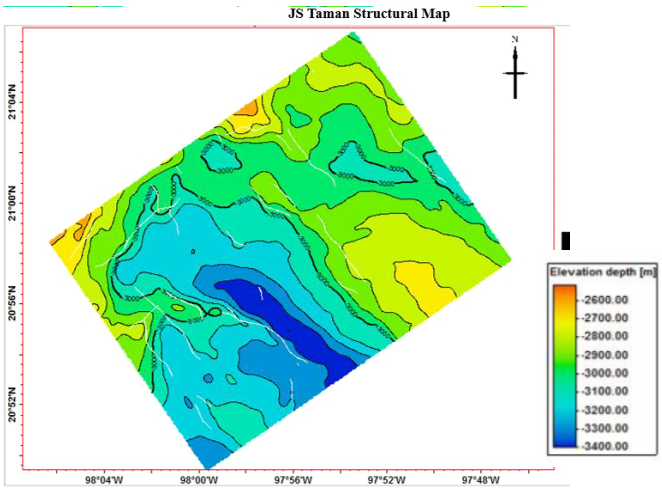

FIGURE 11. Structural map of the top of the Taman Formation. Scale 1–1400000, contour increments 100.

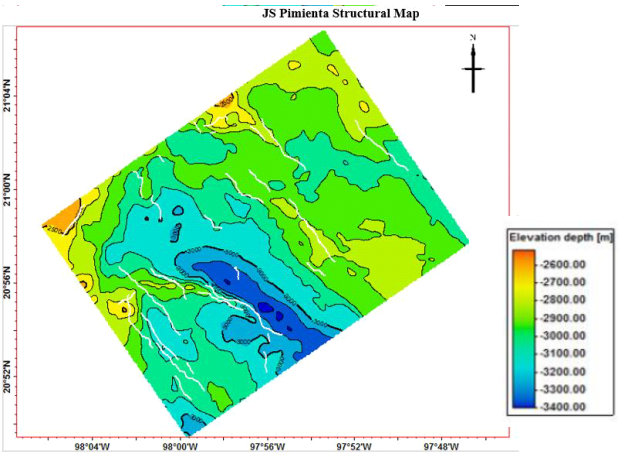

FIGURE 12. Structural map of the top of the Pimienta Formation. Scale 1–1400000, contour increments 100.

limestones and dark gray calcareous shales (Petroleos Mexicanos, 2008). By the end of the Tithonian all depressions had been filled prevailing a passive margin regime that continued until the Santonian.

The Pimienta Formation was deposited in a basin environment to outer ramp setting, marked by high energy processes (Martinez-Yañez *et al.*, 2023). The sedimentary sequence consists of thin layers of black shale, carbonaceous limestone, with intercalations of shale, black and dark brown chert and abundant organic matter (Petroleos Mexicanos, 2008). It shows the surface of maximum marine transgression. Structurally, it is affected by folding and reverse faulting associated with tectonic compression, with NW-SE direction of the structures (Fig. 12).

Seismic attributes

Seismic attributes of the seismic volume give further constraints on the structure and stratigraphy. The RMS and variance attributes are calculated for the basement and top of the Oxfordian, Kimmeridgian and Tithonian Formations.

For the analysis, the attributes are plotted on the structural boundary horizons (Orozco Almazan, 2021; Figs. 13; 14; 15). The seismic attributes at a depth of 6 km in the basement show the RMS and variance attributes display no apparent pattern within the igneous metamorphic basement characterized by scattered orientations. At 5.2km cut-off the RMS attribute shows positive amplitudes over the top of the basement (Fig. 13). Trends show continuity, with horizons marked by high amplitudes at the base of structural heights. It appears the area was subjected to intense erosion with material transported to structural lows. The variance attribute marks steep structural features, coinciding with three major fault zones.

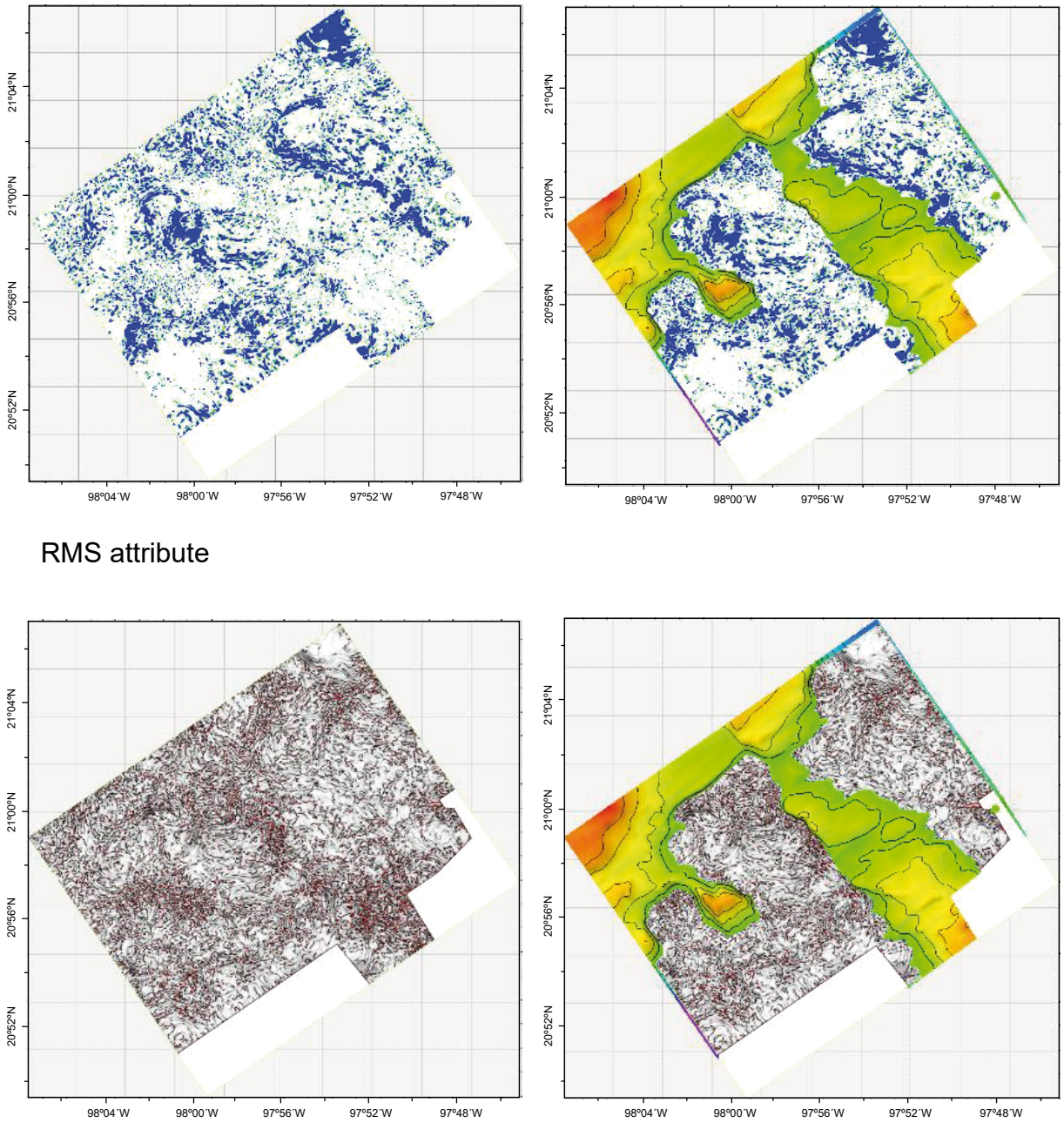

FIGURE 13. Seismic attributes for the basement and top of the Jurassic formations. RMS and variance attributes calculated at cut-off depths of 5.2 km for the basement. The attributes are plotted on the structural boundary horizons.

At 3.7km depth at the top of the Oxfordian formation, the RMS attribute shows large amplitude reflectors, with the variance attribute delineating a fault pattern of three main faults zones. At 3.5km depth at the top of Kimmeridgian Formation the RMS attribute shows a large sediment package in a basin center (Fig. 14). The variance attribute delineates faults coinciding with the flanks of tectonic structures. At 3km depth at the top of the Tithonian formation RMS attribute shows the sediment sequence with high amplitude reflectors in the middle of the large structural basin (Fig. 15). The variance attribute delineates the three fault zones, although at this depth they appear to be less evident. In addition, reduction in number of faults is observed, probably associated with intensity of tectonic activity.

Tri-dimensional models

For visualization, the interpreted horizons are represented in a series of 3-D blocks with considerable vertical exaggeration

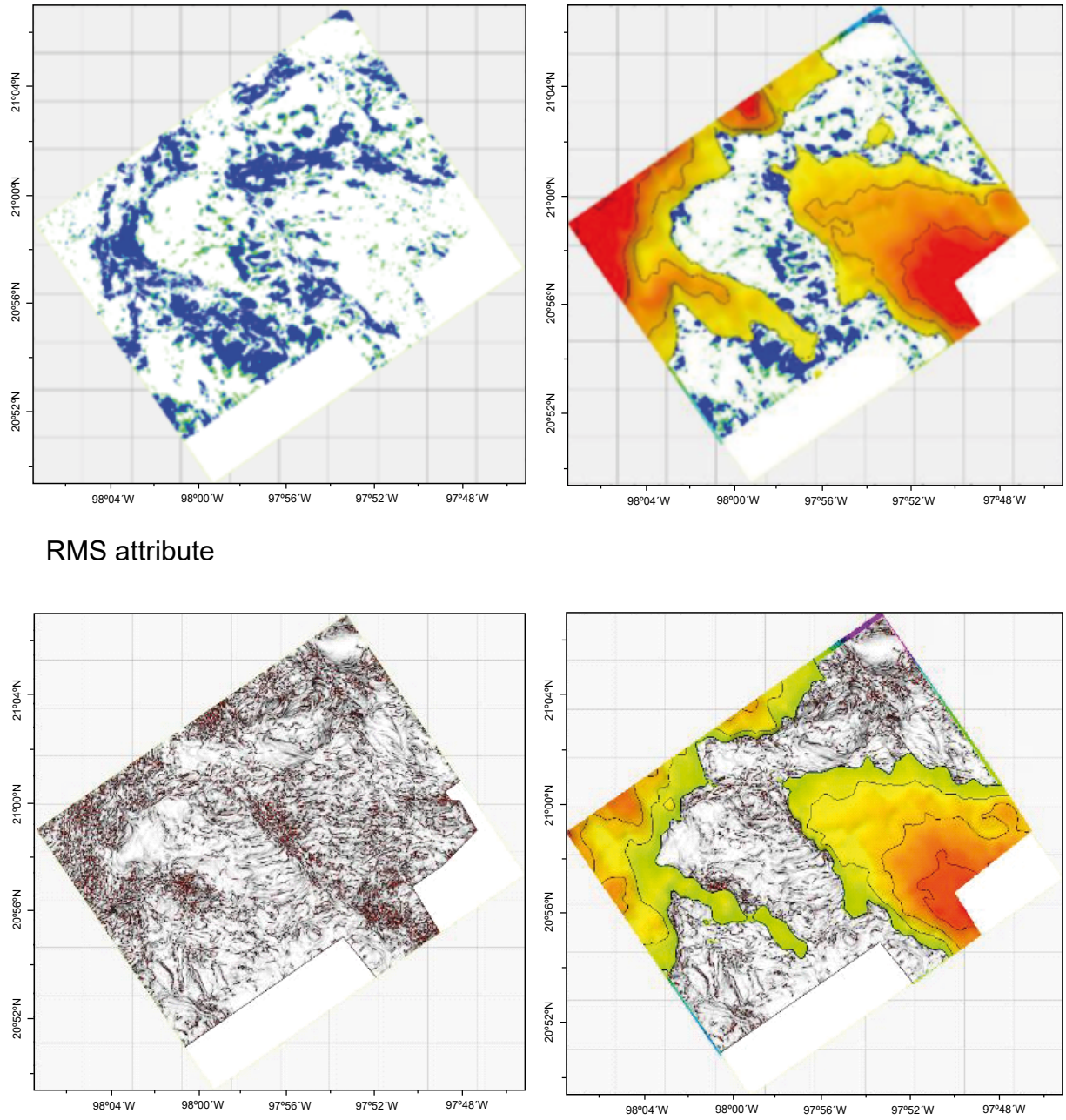

FIGURE 14. RMS and variance seismic attributes calculated at 3.7 km cut-off depth at the top of the Oxfordian. The attributes are plotted on the structural boundary horizons.

(Fig. 16). As noticed, faults planes are not included, rather, the intention is to show relief, lateral thickness variation, vertical and lateral stratigraphic relationships of mapped units. An aspect to highlight is the thinning and eventually pinch out on the Santiago, Taman and Pimienta Formations over the shoulder of structural highs, and the thickening of the Santiago Formation in the Ayacaxtla depression. The 3-D seismic model allows finer subdivision of layers, with constraints on structural relief, thinning, thickening and pinching out of stratigraphic units (Figs. 17-21).

DISCUSSION

The structural and stratigraphic models provide constraints on the structures and sedimentation. Difficult seismic horizons to interpret included the basement, with its top marked by strong amplitude, positive and partially continuous reflections, which in some sectors lie parallel to the Callovian Tepexic and Bajosian top of Cahuasas Formation. The basement horizon is accompanied by a couple of strong amplitude

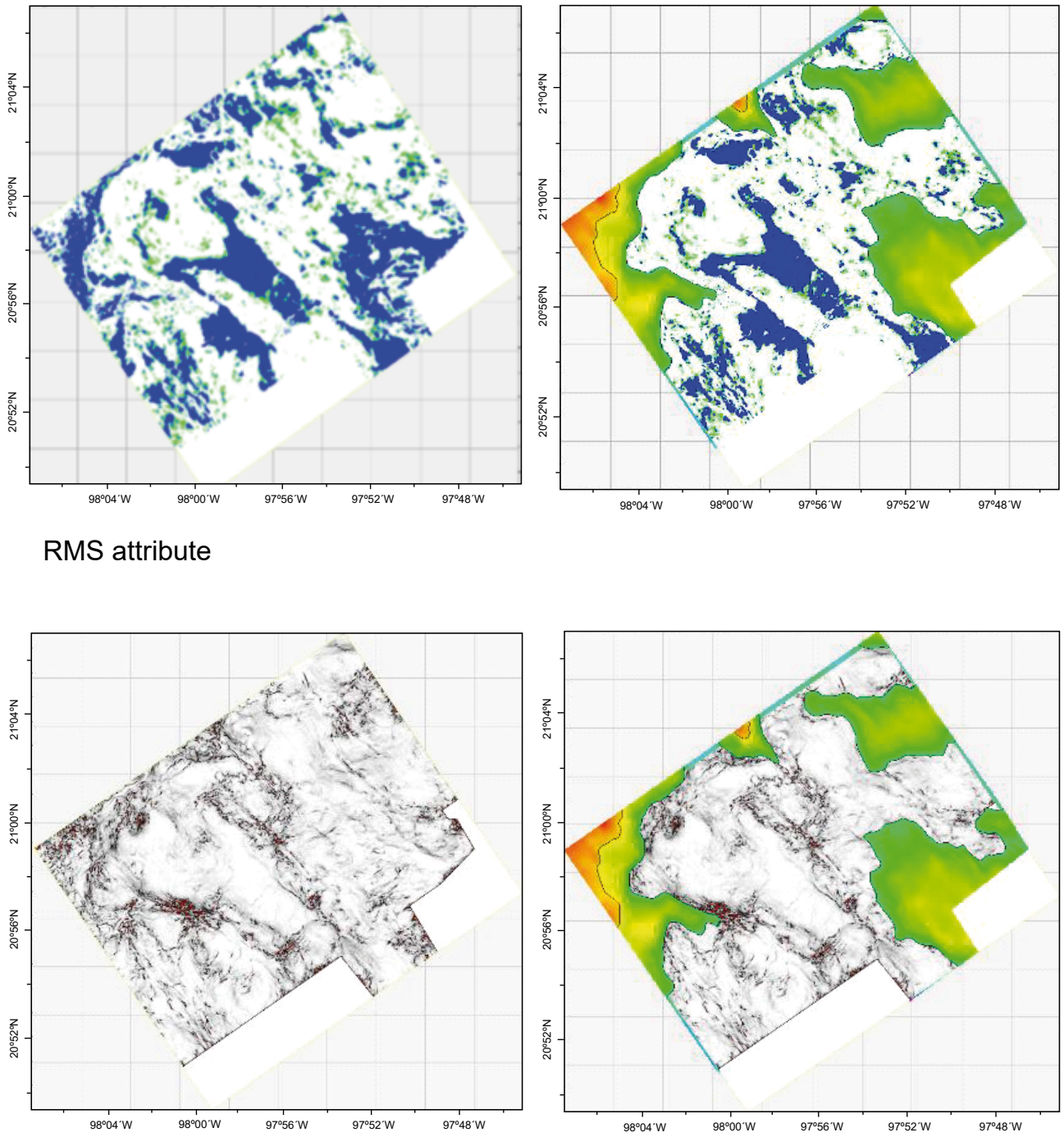

FIGURE 15. RMS and variance attributes calculated for a 3 km cut-off depth at the top of the Tithonian. The attributes are plotted on the structural boundary horizons.

events. Locally, characteristic reflectors are affected by high frequency noise.

The sedimentary sequence between the basement and up to the Middle Jurassic shows considerable thickness, accounting for most of the volume analyzed. From the early rifting stage to until the Callovian, the area was subject to slow sinking and widening of the graben systems that were later inundated. At a 3.0km cut-off at the Tithonian, the upper deposits have an orientation almost parallel to the basal structure with considerable less thickness. Sediments were deposited during the post-rift stage, with a configuration indicating the extensional stresses ceased with basin development was marked by sedimentation. In

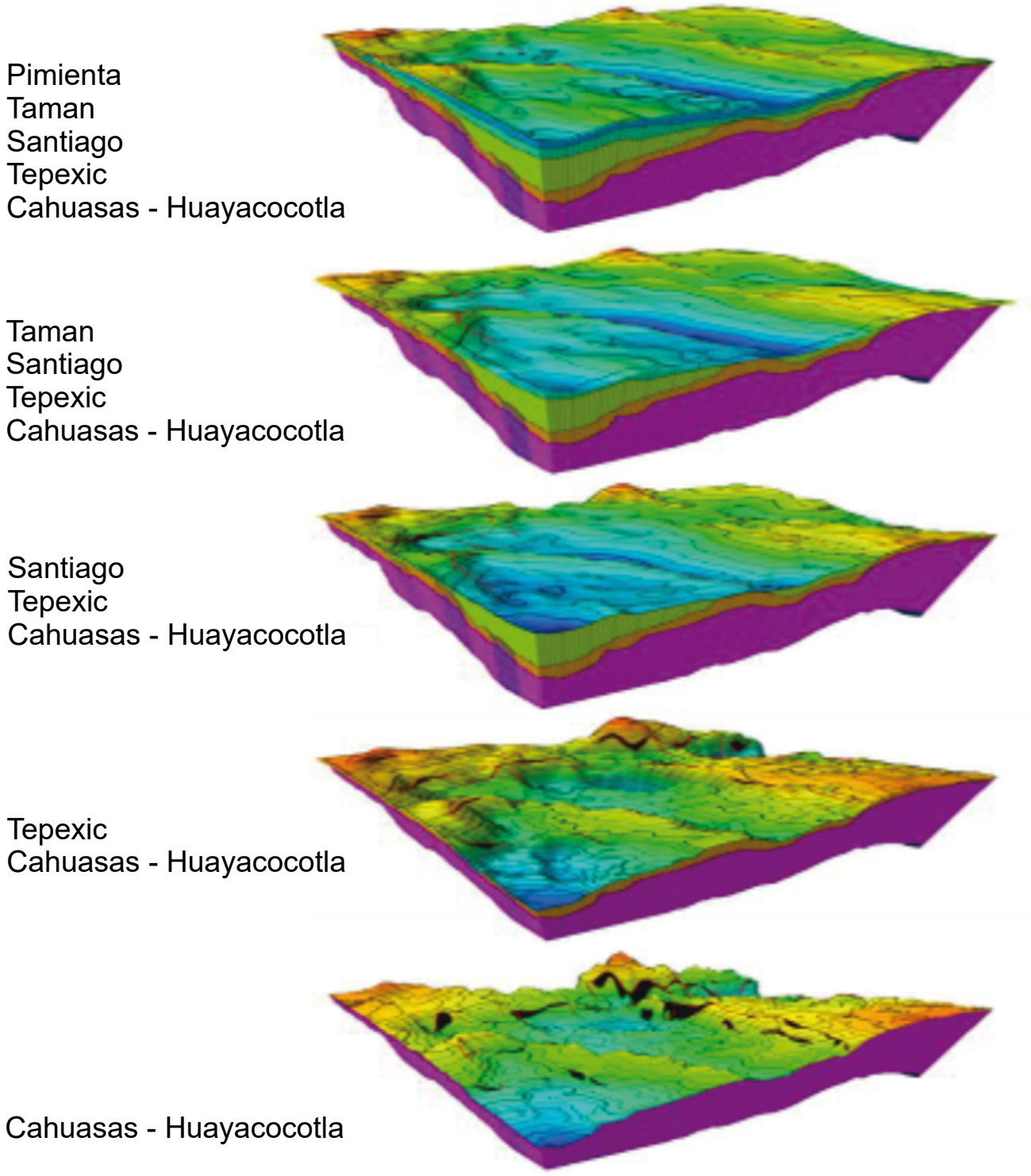

FIGURE 16. 3-D model of the stratigraphic and structural succession of the interpreted formations. Faulting ceased to influence, resulting in a smooth topography as grabens were filled with sediments.

this stage, clastic sediments were derived from basement relief. In the upper sequences, folds and minor faulting are observed, with areas showing normal and inverse faults formed by compressive deformation. In the northern sector, a significant structural low is observed in the basement; The sediments deposited are parallel to the basement

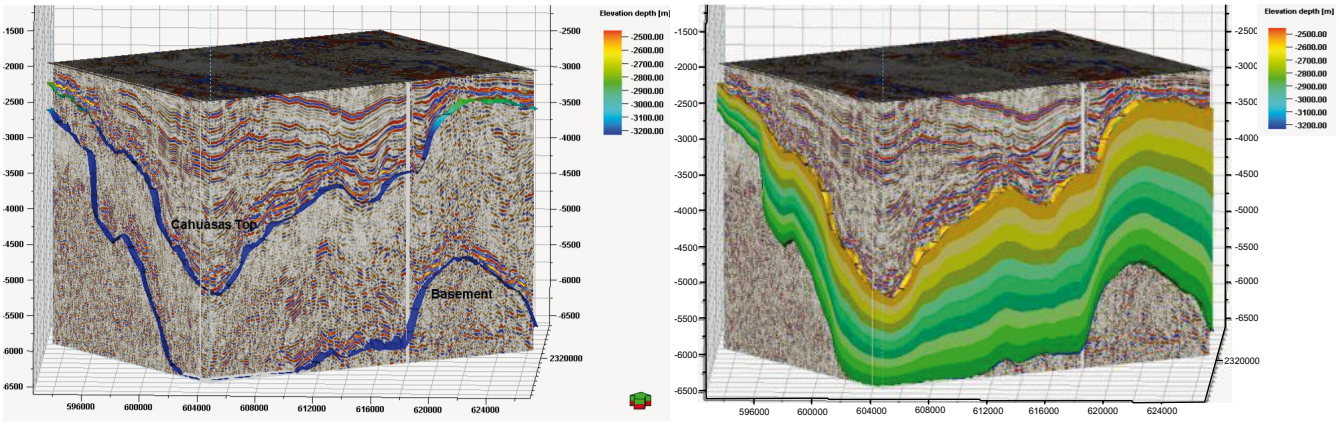

FIGURE 17. Seismic response configuration and interpreted 3-D model between the basement horizon and the top of the Cahuasas Formation.

structure. The upper sedimentary sequence is thicker, filling the structural depression. It can be observed that to the east and west directions, sediment packages decrease their thickness.

Towards the east, the sequence deposited at the base is thick, occupying most of the volume. Therefore, the other two sequences deposited on top get thinner. Towards the NE a structural fosa is identified in the basement, which causes the thickness of the sequence overlying the basement to decrease considerably and the thickness of the two overlying sequences increases, especially the upper sequence that occupies almost all the volume space in this area. To the NE part it can be observed that the upper sequence decreases its thickness until it is wedged with the underlying sequence, whose characteristics correspond to the sin-rift stage. To the south a pronounced structural low is observed, shallower than that in the northern sector. The sequence deposited on the basement is thick, which is followed by a thin sequence practically parallel to it. The upper sequence also has considerable thickness, mostly above the structural basement, thinning to the east and west. The western sector shows minor changes in depth and thickness of sediment packages. The sequence on the basement is of great thickness with less pronounced structural highs and lows. The following sequence is thicker in this part of the volume than at any other, with a distribution almost parallel to the underlying sequence. The upper sequence deposited is thinner, with thickness increasing to the north and south where deeper structural lows are located.

Seismic facies between the two seismic horizons tend to be chaotic and transparent. Although in some zones, high amplitude facies and coherent parallel reflectors are observed. The resulting geometry at the top of the Pimienta preserves the basement morphology of grabens and horsts (Fig. 12). Thickness of 1800m between the basement and Bajosian top of Cahuasas horizons is observed. The stratigraphic column between these two seismic horizons is interpreted to correspond to a rift setting that includes a

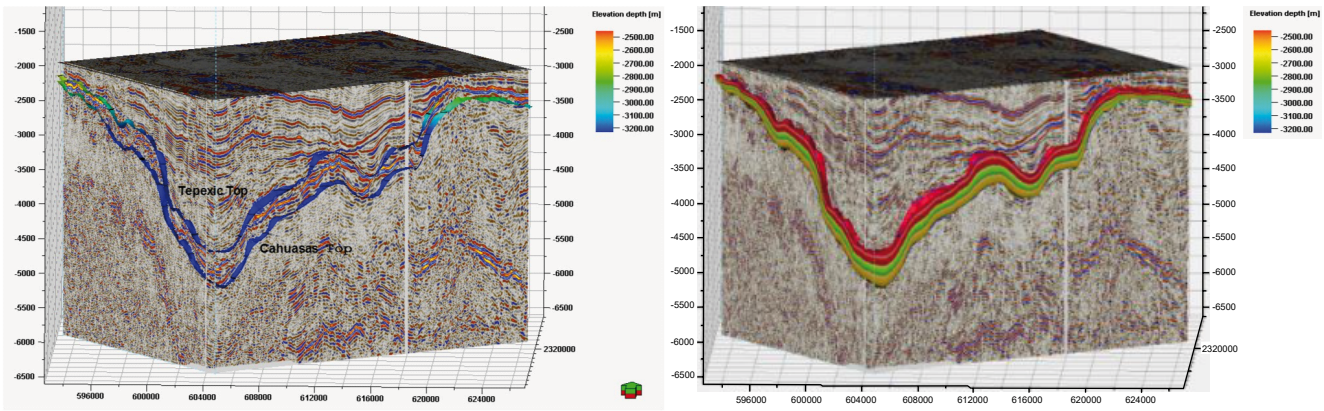

FIGURE 18. Seismic response configuration and interpreted 3-D model between the top horizons of the Cahuasas Formation and Tepexic Formation. Note that the thickness of this sequence is relatively constant.

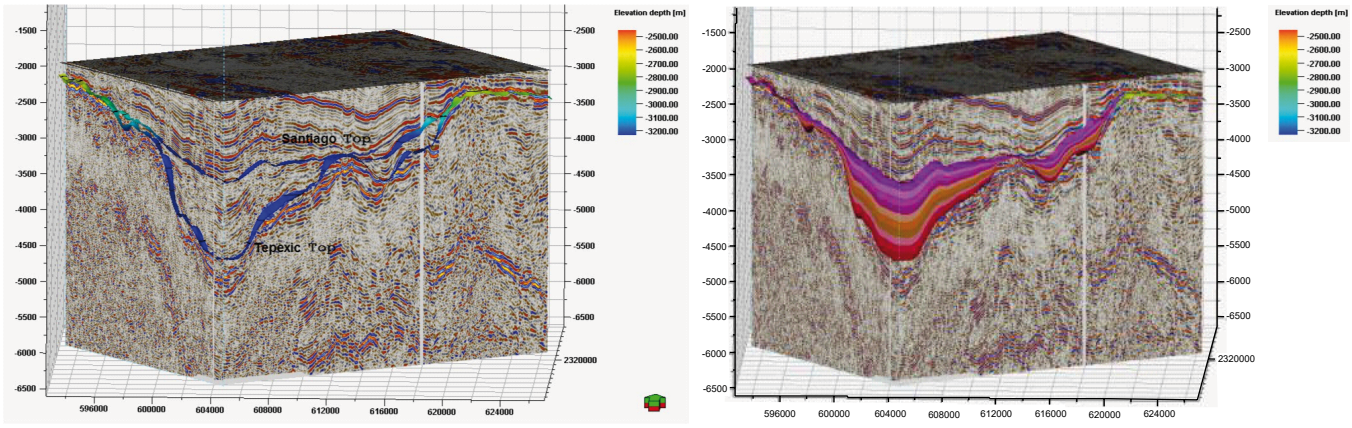

FIGURE 19. Seismic response configuration and interpreted 3-D model between the top horizons of the Tepexic Formation and Santiago Formation. Occurrence of small basins contrasts with the thinning of the layer in other areas, showing differential sedimentation possibly associated with diminished tectonic activity in the region.

thick red bed sequence intruded by igneous rocks, as well as evaporites and shallow marine lower Jurassic sediments of the Huayacocotla Formation. These sequences had been described in northwestern Gulf of Mexico as deposited in a rift setting from late Triassic to earliest Oxfordian (Goldhammer and Johnson, 2001; Goldhammer *et al.*, 1991).

In the study area we propose that rifting stage ceased by the end of Bajosian, and that Callovian sediments represented by the Tepexic and Huehuetepc formations were deposited during transition from rift to passive margin regimes as sag deposits. This is consistent with interpretation of the widespread seismic sequence of relatively high acoustic impedance, associated with evaporites and shallow marine deposits of the Huehuetepec and Tepexic formations. Thermal subsidence and thickness changes are expected, with a thicker sequence over the rift axis.

3-D models permit to constraint the structure and stratigraphy of sedimentary units and relationships with the basement. Models quantify thickness and seismic reflection packages. Deposits of the Cahuasa Formation follow the basement relief, with varying thickness (Santiago/Taman contact surface (Fig. 17). Figure 18 shows the sedimentary deposits for the Tepexic Formation and Cahuasas/Tepexic contact surface. The deposits and contact surface for the Tepexic/Santiago are shown in Figure 19. Deposits of the Oxfordian Santiago Formation formed thick wedges that pinch out against paleogeographic relief, reflected in the Santiago/Taman contact surface (Fig. 20). Deposits of the Taman Formation and Taman/Pimienta contact surface is shown in Figure 21.

A deep basement has significant impact on the thermal and subsidence history of the Tampico-Misantla basin. The basement structures controlled the geometry, distribution and lateral variations of overlaying Jurassic units. Basement

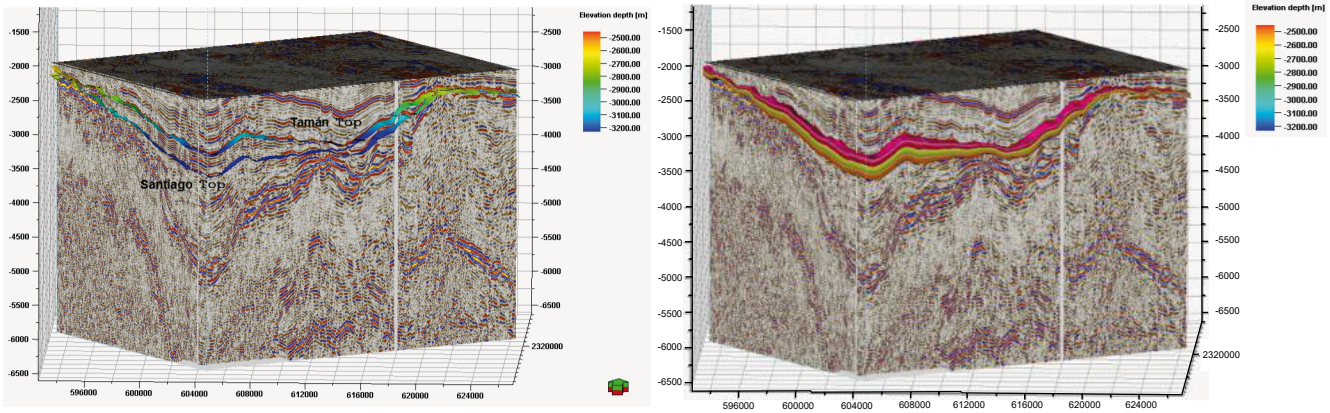

FIGURE 20. Seismic response configuration and interpreted 3-D model between the top horizons of the Santiago Formation and Tamán Formation. Both the top and base of the sequence are nearly parallel to each other.

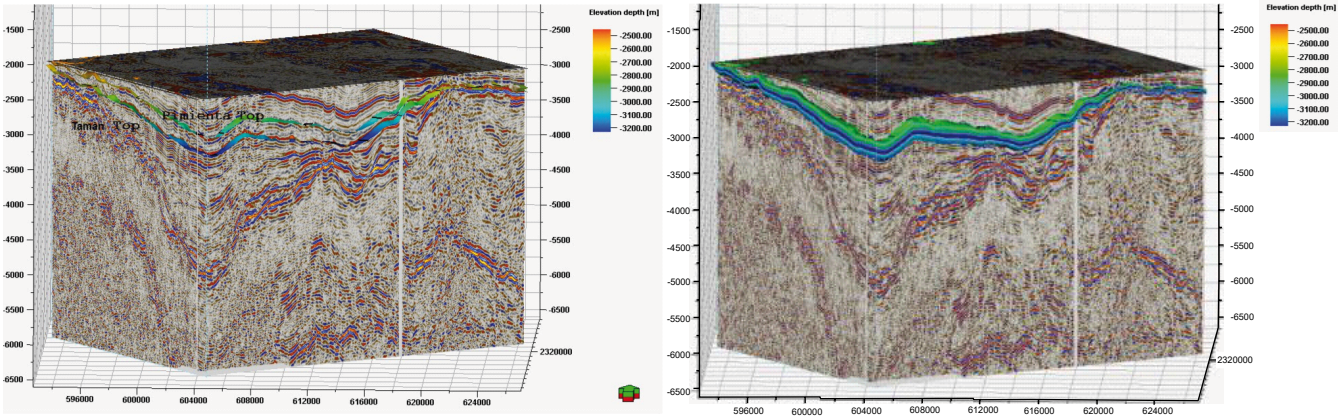

FIGURE 21. Seismic response configuration and interpreted 3-D model between the top horizons of the Taman Formation and Pimienta Formation. Although it is a sequence almost parallel to its predecessor, it shows a smoother topography, indicating more stable tectonic conditions.

complex arrangements of horsts and grabens resulted from the rifting process that took place from Triassic to Middle Jurassic. The sediment infills of low relief regions were mostly continental, with variable thickness from block to block. Faults limiting blocks are high angle, planar and curved with large vertical slips. Fault orientations and blocks arrangement relate to the stress directions.

An interesting feature is the widespread presence of a seismic package of relatively uniform thickness and high acoustic impedance related to the Callovian Huehuetepec and Tepexic formations. The base of the Huehuetepec Formation marks the culmination of both, the rifting stage and the infilling process of grabens with sediments of the Cahuasas Formation.

The fault reactivations that bound horsts, grabens and subsidence produced localized depocenters over former grabens that caught sediments form the Santiago, Taman and Pimienta Formations. At the same time, these units wedged out against remaining highs, with depressions filled by the end of Tithonian. Finally, compression during the Laramide orogeny produced folding and fault reactivation (Fitz-Diaz *et al.*, 2018). In some cases, compressional deformation inverted them from normal to reverse, affecting the upper Jurassic and Cretaceous units. Representation of stratigraphic units as multiple proportional layers helps to visualize their stratigraphic behavior, *i.e.* lateral extent, thickness variations and pinch outs.

Geomorphological analysis of the Tamán and Pimienta seismic units suggests deposition under tectonically stable subsidence, widespread and uniform sedimentation in relatively shallow basins. Although, subtle pinch outs against paleo-topographic highs, as remnants of the basement top, are observed (Figs. 11; 12). The complex patterns of tectonism and sedimentation occurred during regional and complex divergent processes, resulting in the Pangea break up and opening of the Gulf of Mexico (Bird *et al.*, 2005; Goldhammer *et al.*, 2001; Goldhammer *et al.*, 2015; Salvador, 1987, 1991).

Oblique 3-D views of the seismic models for the Jurassic formations, (Tithonian) Pimienta, (Kimmeridigian) Taman/San Andrés, (Oxfordian) Santiago, (Callovian) Tepexic/Huehuetepec and (Bathonian) Cahuasas are summarized in Figures 17 to 21. Influence of basement structures appear dominant in rift sequences. Rift faulting patterns respond to the stress field, with the influence of basement structures that define local deformation and fault reactivation (Strugale *et al.*, 2021).

CONCLUSIONS

The Tampico-Misantla Basin sedimentary sequences in the northern sector of the Chicontepec Basin show approximate thickness of 4,000meters. Study defines four seismic packages corresponding to the Jurassic Formations and three fault systems, associated with tectonic events with the Pangaea breakup and the opening of the Gulf of Mexico. The comparison of the 3-D models, RMS and variance seismic attributes and structural maps constraints the configuration of the basement and Jurassic formations, with the extent and thickness of the sedimentary sequences.

The seismic models allow characterization of the structural and stratigraphic features associated with the basement and Jurassic sedimentary formations. For the analysis, the basement and stratigraphic horizons for the Tithonian Pimienta, Kimmeridigian Taman and San Andrés, Oxfordian Santiago, Callovian Tepexic and Huehuetepec and Bathonian Cahuasas formations

are defined from the seismic data. The basement is characterized by stepped NW-SE tilted blocks of horst and grabens, limited by planar and curved, high angle normal faults with NW-SE and NE-SW orientation forming a conjugated system. Vertical slips of main faults are variable and may reach 2000m. The basement blocks play a major role in defining the depositional systems, with the thickness and distribution of overlying sedimentary units. Based on our analysis the middle Jurassic stratigraphic units of the Cahuasas Formation were deposited predominantly in continental environments and exhibit large thickness variations from block to block. The Callovian Tepexic and Huehuetepec Formations were deposited in transitional and shallow marine environments, with relatively uniform thickness and distribution. The Oxfordian to Tithonian Santiago, Taman/San Andres and Pimienta Formations were deposited in varying marine environments, showing a tendency to progressively pinch out against the paleotopographic highs. The significant thickness variation in the Santiago Formation suggests episodes of increasing subsidence and fault reactivation.

Two episodes of extension associated with normal faulting and subsidence are interpreted, during a rifting stage from Triassic to middle Jurassic and during the Oxfordian in a passive margin regime. The episodes are separated by a period of deposition of evaporites and shallow marine sediments that mark the first pulses of marine invasion into the Tampico-Misantla basin and the transition between rifting and passive margin stages. Reactivation of normal faults and localized subsidence that gave place to wedge shape deposits occurred during the Oxfordian and continued with less intensity until the end of the Tithonian. Some faults were reactivated and inverted to reverse faults during the late Cretaceous-middle Eocene Laramide orogeny.

The seismic study documents the structure and stratigraphy of the basement and sedimentary formations, with the seismic horizons associated with tectonics and deposition of the Jurassic sequences in the Tampico-Misantla basin in northeastern Mexico.

CONFLICT OF INTERESTS

Authors declare that they have no known competing financial or conflicts of interest related to this study.

DATA

The seismic data set used in this study is available in the National Hydrocarbon Commission CNH database.

ACKNOWLEDGMENTS

We thank the editor and journal reviewers for insightful revision of the manuscript and editorial assistance. We acknowledge access to the Petroleos Mexicanos seismic data for the Tampico-Misantla Basin study area from the CNH National Hydrocarbon Commission, Mexico. We thank Dr. Victor Luna for assistance with the project. We acknowledge the collaboration and useful discussions with Dr. Ligia Perez Cruz. This is publication IICEAC 2025-06.

REFERENCES

Abascal-Hernández, G., León-Francisco, J., Torres-Vargas, R., Garduño-Martínez, D., Franco-Navarrete, S., Méndez-Vázquez, J., Ortega-Lucach, S., Gutiérrez-Caminero, L., Murillo-Muñetón, G., 2018. Sedimentological characterization of the Pimienta Formation in the central part of the Tampico-Misantla Basin, Veracruz, Mexico. In SPE/AAPG/SEG Unconventional Resources Technology Conference (p. D023S025R009). URTEC.

Aguilera, H.E., 1972. Ambientes de depósito de las formaciones del Jurásico Superior en la región Tampico Tuxpan. Boletin Asociacion Mexicana Geologos Petroleros, 24(1-3), 129-163.

Assis, C.A., Santos, H.B., Schleicher, J., 2019. Colored and linear inversions to relative acoustic impedance. Geophysics, 84(2), N15-N27.

Bird, D.E., Burke, K., Hall, S.A., Casey, J.F., 2005. Gulf of Mexico tectonic history: Hotspot tracks, crustal boundaries, and early salt distribution. AAPG Bulletin, 89(3), 311-328.

Busch, D.A., Govela, S.A., 1978. Stratigraphy and structure of Chicontepec turbidites, southeastern Tampico-Misantla Basin. AAPG Bulletin, 62, 235-246.

Cantú-Chapa, A., 1969. Estratigrafía del Jurásico Medio-Superior del Subsuelo de Poza Rica, Ver. (área de Soledad-Miquetla). Revista Instituto Mexicano Petroleo, 1(1), 3-9.

Cantú-Chapa, A., 1984. El Jurásico Superior de Tamán, San Luis Potosí, Este de México. III Congreso Latinoamericano Paleontologia Memoria, 207-212.

Carrillo-Bravo, J., 1971. La Plataforma de Valles-San Luis Potosí. Boletin Asociacion Mexicana Geologos Petroleros, 23(1-6), 1-102.

Chopra, S., Marfurt, K.J., 2005. Seismic attributes—A historical perspective. Geophysics, 70(5), 3SO-28SO.

Chopra, S., Marfurt, K.J., 2018. Coherence attribute applications in seismic data in various guises – Part 1. Interpretation, 6(3), T521-T529.

Comisión Nacional de Hidrocarburos, 2018. Atlas Geólogico Cuenca Tampico Misantla, Comision Nacional de Hidrocarburos CNH, Mexico.

Fitz-Díaz, E., Lawton, T.F., Juárez-Arriaga, E., Chávez-Cabello, G., 2018. The Cretaceous–Paleogene Mexican orogen: Structure, basin development, magmatism and tectonics. Earth-

Science Reviews, 183, 56-84. DOI: https://doi.org/10.1016/j.earscirev.2017.03.002

Goldhammer, R.K., 1999. Mesozoic sequence stratigraphy and paleogeographic evolution of northeast Mexico. In: Bartolini, C., Wilson, J.L., Lawton, T.F. (eds.). Geological Society America Special Paper, 340, DOI: https://doi.org/10.1130/0-8137-2340-X.1

Goldhammer, R.K., Johnson, C.A., 2001. Middle Jurassic-Upper Cretaceous paleogeographic evolution and sequence stratigraphic framework of the northwest Gulf of Mexico rim. The Western Gulf of Mexico Basin: Tectonics, Sedimentary Basins, and Petroleum Systems AAPG Memoir, 75, 45-81.

Goldhammer, R.K., Lehman, P.J., Todd, R.G., Wilson, J.L, Ward, W.C., Johnson, C.R., 1991. Sequence stratigraphy and cyclostratigraphy of the Mesozoic of the Sierra Madre Oriental, northeast Mexico, a field guidebook. SEPM Gulf Coast Section, 85pp.

Gonzalez-García, R., 1970. La Formación Huehuetepec, nueva unidad litoestratigráfica del Jurásico de Poza Rica. Asociacion Ingenieros Petroleros México, Revista Ingenieria Petrolera, 10(7), 5-22.

Gray, G.G., Pottorf, R.J., Yurewicz, D.A., Mahon, K.I., Pevear, D.R., Chuchla, R.J., 2001. Thermal and chronological record of syn- to post Laramide burial and exhumation, Sierra Madre Oriental, Mexico. In: Bartolini, C., Buffler, R.T., Cantu-Chapa, A. (eds.). The Western Gulf of Mexico Basin: Tectonics, Sedimentary Basins, and Petroleum Systems: American Association of Petroleum Geologists Memoir 75, 159-181. DOI: https://doi.org/10.1306/M75768C7

Gray, S.H., Etgen, J., Dellinger, J., Whitmore, D., 2001. Seismic migration problems and solutions. Geophysics, 66(5), 1622-1640.

Guzman, A.E., 2022. Tampico-Misantla: A premier super basin in waiting. AAPG Bulletin, 106(3), 495-516.

Guzman-Vega, M.A., L. Castro Ortiz, J.R., Roman Ramos, L., Medrano Morales, L.C., Valdez, E., Vazquez-Covarrubias, Ziga Rodriguez, G., 2001. Classification and origin of petroleum in the Mexican Gulf Coast Basin: An overview. In: Bartolini, C., Buffler, R.T., Cantu-Chapa, A. (eds.). The western Gulf of Mexico Basin: Tectonics, sedimentary basins, and petroleum systems: AAPG Memoir 75, 127-142.

Hart, B., 2008. Stratigraphically significant attributes. The Leading Edge, 27(3), 320-324.

Heim, A., 1926. Notes on the Jurassic of Tamazunchale (Sierra Madre Oriental, México). Eclogae Geologica Helvetiae, 20(1), 84-87.

Heim, A., 1940. The From Ranges of Sierra Madre Oriental, Mexico, from Ciudad Victoria to Tamazunchale. Eclogae Geologica Helvetiae, 33, 315-352.

Hermoso de La Torre, C., Martínez-Pérez, J., 1972. Medición detallada de formaciones del Jurásico Superior en el frente de la Sierra Madre Oriental. Boletin Asociacion Mexicana Geologos Petroleros, 24(1-3), 45-63.

Jarvie, D., Maende, A., 2016. Mexico's Tithonian Pimienta Shale: Potential for unconventional production. Society of Petroleum Engineers/AAPG/Society of Exploration Geophysicists Unconventional Resources Technology Conference, San Antonio, Texas, August 1–3, 2016, URTEC-2016-2433439, doi:10.15530/urtec-2016-2433439.

Jarvie, D.M., 2012. Shale resource systems for oil and gas: Part 2—Shale-oil resource systems. In: Breyer, J.A. (ed.). Shale Reservoirs—Giant Resources for the 21st Century. AAPG Memoir, 97, 89-119.

Karimi, P., 2015. Structure-constrained relative acoustic impedance using stratigraphic coordinates. Geophysics, 80(3), A63-A67.

López-Infanzón, M., 1986. Estudio petrogenético de las rocas ígneas en las formaciones Huizachal y Nazas. Boletin Sociedad Geologica Mexicana, 47(2), 1-42.

López-Ramos, E., 1979. Geología de México, Tomo II, 2da. Edición, México, D.F., 454 p.

Maende, A., 2016. Wildcat compositional analysis for conventional and unconventional reservoir assessments. HAWK Petroleum Assessment Method (H-PAM), Application Note 052016-1, 11pp. Website: http://www.wildcattechnologies.com/download_file/view/136/358.

Magoon, L.B., Hudson, T.L., Cook, H.E., 2001. Pimienta-Tamabra(!) - a giant supercharged petroleum system in the southern Gulf of Mexico, onshore and offshore Mexico. Bartolini, C., Buffler, R.T., Cantú-Chapa, A. (eds.). The Western Gulf of Mexico Basin. Tectonics, Sedimentary Basins, and Petroleum Systems, 75, 83-125. DOI: 10.1306/M75768C4

Marfurt, K.J., 2007. Seismic attributes for prospect identification and reservoir characterization. In: Chopra, S., European Association of Geoscientists & Engineers, Society of Exploration Geophysicists, 464pp.

Martínez-Yáñez, M., Núñez-Useche, F., Enciso Cárdenas, J.J., Omaña, L., Colín-García, M., de la Rosa-Rodríguez, G., Ruiz-Correa, A., Mesa-Rojas, J.L., 2023. Environmental controls on the microfacies distribution and spectral gamma ray response of the uppermost Jurassic–Lowermost Cretaceous succession (Pimienta–Lower Tamaulipas Formations) in central-eastern Mexico. Journal South American Earth Sciences, 124, 104240.

Medina, E., 2023. A basin scale assessment framework of onshore aquifer-based CO_2 suitability storage in Tampico Misantla basin, Mexico. International Journal Greenhouse Gas Contributions, 125.

Morelos Garcia, J.A.M., 1996. Geochemical evaluation of southern Tampico-Misantla basin, Mexico. Oil-oil and oil source rock correlations. Ph.D. Thesis. The University of Texas at Dallas, 635pp.

Muir, J.M., 1936. Geology of the Tampico Region, Mexico. AAPG, p. 4, DOI: 10.1306/SV8338

Orozco Almazan, L., 2021. Alcances estructurales en la apertura del rift en la distribución de yacimientos no convencionales, en una porción de la cuenca Tampico Misantla. Tesis Ingenieria Geofisica Facultad de Ingenieria, Universidad Nacional Autonoma de Mexico, Mexico

Petróleos Mexicanos, 1988. Estratigrafía de la República Mexicana: Mesozoico, Petroleos Mexicanos, Pemex Subdirección de Producción Primaria, Coordinación Ejecutiva de Exploración, Mexico, 229pp.

Petróleos Mexicanos, 2008. Reservas de hidrocarburos, In: Pemex Memoria de Labores 2007, Petroleos Mexicanos, Mexico.

Ranson, W.A., Fernández, L.A., Simmons, W.B., Enciso De La Vega, S., 1982. Petrology of the metamorphic rocks of Zacatecas, Zac., Mexico. Boletin Sociedad Geologica Mexicana, 43(1), 37-59.

Salguero-Hernández, E., Pérez-Cruz, L., Urrutia-Fucugauchi, J., 2020. Seismic attribute analysis of Chicxulub impact crater. Acta Geophysica, 68, 627-640.

Salvador, A., 1987. Late Triassic–Jurassic paleogeography and origin of Gulf of Mexico Basin. Am. Assoc. Petrol. Geol. Bull., 71, 419-451.

Salvador, A., 1991. Triassic-Jurassic. In: Salvador, A. (ed.). The Gulf of Mexico Basin. Boulder (Colorado), Geol. Soc. Am., The Geologic of North America, J., 131-180.

Strugale, M., da Silva Schmitt, R., Cartwright, J., 2021. Basement geology and its controls on the nucleation and growth of rift faults in the northern Campos Basin, offshore Brazil. Basin Research, 33(3), 1906-1933.

Van Avendock, H.J., Christeson, G.L., Norton, I.O., Eddy, D.R., 2015. Continental rifting and sediment infill in the northwestern Gulf of Mexico. Geology, 43(7), 631-634.

Vega-Ortiz, C., Beti, D.R., Setoyama, E., McLennan, J.D., Ring, T.A., Levey, R., Martinez-Romero, N., 2020. Source rock evaluation I the central-western flank of the Tampico-Misantla basin, Mexico. Journal South American Earth Sciences, 100, 102552.

White, R.E., 1991. Properties of instantaneous seismic attributes. The Leading Edge, 10(7), 26-32.

Wilson, J.L., 1986. Basement structural controls on Mesozoic carbonate facies in northeastern Mexico—a review. Carbonate Platforms: Facies, Sequences and Evolution, 235-255.

Manuscript received Month year;
revision accepted Month year;
published Online October 2025.